

LETTER • OPEN ACCESS

Recent multispecies tree-growth decline reveals a severe aridity change in Mediterranean Chile

To cite this article: Álvaro González-Reyes *et al* 2024 *Environ. Res. Lett.* **19** 064046

View the [article online](#) for updates and enhancements.

You may also like

- [The 'Day Zero' Cape Town drought and the poleward migration of moisture corridors](#)
Pedro M Sousa, Ross C Blamey, Chris J C Reason *et al.*
- [Decoupling environmental water markets from water law](#)
Philip Womble, Allen Townsend and Leon F Szeptycki
- [Increased wildfire hazard along South-Central Chile under the RCP8.5 scenario as revealed by high-resolution modeling](#)
Isabella Ciocca, Alfonso Fernández, Edilia Jaque *et al.*

Breath Biopsy Conference

BREATH
BIOPSY

Join the conference to explore the **latest challenges** and advances in **breath research**, you could even **present your latest work!**



5th & 6th November
Online



Main talks



Early career sessions



Posters

Register now for free!

ENVIRONMENTAL RESEARCH
LETTERS

LETTER

Recent multispecies tree-growth decline reveals a severe aridity change in Mediterranean Chile

OPEN ACCESS

RECEIVED

2 December 2023

REVISED

21 February 2024

ACCEPTED FOR PUBLICATION

18 April 2024












PUBLISHED

24 May 2024

Original content from this work may be used under the terms of the [Creative Commons Attribution 4.0 licence](#).

Any further distribution of this work must maintain attribution to the author(s) and the title of the work, journal citation and DOI.



Álvaro González-Reyes^{1,2,3,4,*} , Duncan A Christie^{3,5,6,7} , Isadora Schneider-Valenzuela^{8,9,10} , Alejandro Venegas-González¹¹ , Ariel A Muñoz^{6,8,9,12} , Martín Hadad¹³ , Tania Gipoulou-Zuñiga³ , Valeria Tapia-Marzan⁸, Stephanie Gibson-Carpintero¹¹ , Luiz Santini-Junior¹⁴ , Carlos LeQuesne^{3,5} , and Ricardo Villalba¹⁵ 

¹ Instituto de Ciencias de la Tierra, Facultad de Ciencias, Universidad Austral de Chile, Valdivia, Chile

² Centro de Humedales río Cruces CEHUM, Universidad Austral de Chile, Valdivia, Chile

³ Laboratorio de Dendrocronología y Cambio Global, Universidad Austral de Chile, Valdivia, Chile

⁴ Centro FONDAPE de Investigación de Dinámicas de Ecosistemas Marinos de Altas Latitudes (IDEAL), Valdivia, Chile

⁵ Instituto de Conservación Biodiversidad y Territorio, Universidad Austral de Chile, Valdivia, Chile

⁶ Center for Climate and Resilience Research (CR)², Santiago, Chile

⁷ Cape Horn International Center (CHIC), Parque Etnobotánico Omora, Universidad de Magallanes, Puerto Williams, Chile

⁸ Laboratorio de Dendrocronología y Estudios Ambientales, Instituto de Geografía, Pontificia Universidad Católica de Valparaíso, Valparaíso, Chile

⁹ Centro de Acción Climática, Pontificia Universidad Católica de Valparaíso, Valparaíso, Chile

¹⁰ Programa de Doctorado en Ciencias mención Ecología y Biología Evolutiva, Facultad de Ciencias, Universidad de Chile, Las Palmeras 3425, Santiago, Nuñoa 7750000, Chile

¹¹ Instituto de Ciencias Agroalimentarias, Animales y Ambientales (ICA3), Universidad de O'Higgins, San Fernando, Chile

¹² Centro Regional de Investigación e Innovación para la Sostenibilidad de la Agricultura y los Territorios Rurales CERES, Pontificia Universidad Católica de Valparaíso, Quillota, Valparaíso 2260000, Chile

¹³ Laboratorio de Dendrocronología de Zonas Áridas. CIGEOBIO (CONICET-UNSA), San Juan, Argentina

¹⁴ Grupo de Pesquisa em Ecologia Florestal, Instituto de Desenvolvimento Sustentável Mamirauá, Tefe, Amazonas, Brazil

¹⁵ Laboratorio de Dendrocronología e Historia Ambiental, IANIGLA-CCT CONICET, Mendoza, Argentina

* Author to whom any correspondence should be addressed.

E-mail: alvaro.gonzalez@uach.cl

Keywords: soil moisture, growth decline, Mediterranean Chile, drought stress

Supplementary material for this article is available [online](#)

Abstract

Soil moisture (SM) is a crucial factor in the water cycle, sustaining ecosystems and influencing local climate patterns by regulating the energy balance between the soil and atmosphere. Due to the absence of long-term, *in-situ* measurements of SM, studies utilizing satellite-based data and tree-ring analysis have become valuable in assessing variations of SM at regional and multi-century scales, as well as determining its effects on tree growth. This information is particularly pertinent in biodiversity hotspots made up of semi-arid ecosystems currently threatened by climate change. In the Mediterranean Chile region (MC; 30°–37° S), an ongoing megadrought since 2010 has resulted in a significant decline in the forest throughout the area. However, the impact of SM on tree growth at a multi-species and regional level remains unexplored. We analyzed a new network of 22 tree-ring width chronologies across the MC to evaluate the main spatiotemporal tree-growth patterns of nine woody species and their correlation with SM, using PCA. We also reconstructed the SM variations over the past four centuries and assessed its connection with large-scale climate forcings. Our results indicate that the primary growth patterns (PC1) explained 27% of the total variance and displayed a significant relationship with SM between 1982–2015 ($r = 0.91$), accurately reflecting the current megadrought. The tree-ring SM reconstruction covers the period 1616–2018 and shows a strong decrease around the year 2007, revealing an unprecedented recent change in aridity with respect to the last four centuries. The intensity of the South Pacific subtropical anticyclone, which primarily owe their existence to the subsiding branch of the Hadley

Cell, appears as the primary climatic mechanism correlated with the reconstruction and the present aridity conditions in MC. The current SM conditions align with anticipated aridity changes in MC, providing a bleak perspective of future regional climate.

1. Introduction

Many sub-tropical regions are currently facing significant environmental changes influenced by the increased frequency, duration, and intensity of droughts (Allen *et al* 2015, McDowell *et al* 2020, Cook *et al* 2022). These changes affect the availability of water resources and the dynamics of forest ecosystems, with implications for carbon and hydrological dynamics (Anderegg *et al* 2015, Kannenberg *et al* 2019, Forzieri *et al* 2022). Located in the subtropical western coast of South America, the Mediterranean region of Central Chile (MC; 30°–37° S) is considered a global biodiversity hotspot, and one of the biologically richest and most endangered terrestrial ecosystems on Earth (Mittermeier *et al* 2011, Fuentes-Castillo 2020). The MC biome contributes to the balance of carbon storage and water regulation in a highly anthropic region that concentrates over 70% of the country's population and is the primary contributor to national agricultural production (Cerdeña *et al* 2014, Roco *et al* 2015, Montoya-Tangarife *et al* 2017). MC has a high biodiversity and endemism level of flora and fauna (Myers *et al* 2000), but several studies have reported a significant increase in risk factors threatening it, including widespread land-use change (Schulz *et al* 2010, Uribe *et al* 2020), human-caused fires (Urrutia-Jalabert *et al* 2018, Bowman *et al* 2020), and the current megadrought (Garreaud *et al* 2017, 2020), partly attributable to anthropogenic forcings (Boisier *et al* 2018). This unprecedented event coincides with an increase in air temperature (Burger *et al* 2018) and a decrease in precipitation in recent decades (Rivera *et al* 2017, Garreaud *et al* 2020), which has caused a massive regional decline in sclerophyll forest ecosystems (Venegas-González *et al* 2019, 2023, Miranda *et al* 2020). Climate models suggest that aridity conditions will intensify in this region during the 21st century, negatively impacting tree growth (Matskovsky *et al* 2021) and species distribution (Fuentes-Castillo *et al* 2019). This will further enhance the vulnerability of biodiversity, ecosystem services, and regional economies in the MC region (Schwabe *et al* 2013).

Assessing the variability of soil surface water balance is crucial for understanding the environmental impacts of droughts and for assessing possible ongoing climatic changes in densely populated and endangered ecosystems of subtropical semi-arid regions. Tree rings in Mediterranean regions are recognized for their ability to document hydroclimatic conditions at interannual, decadal, and

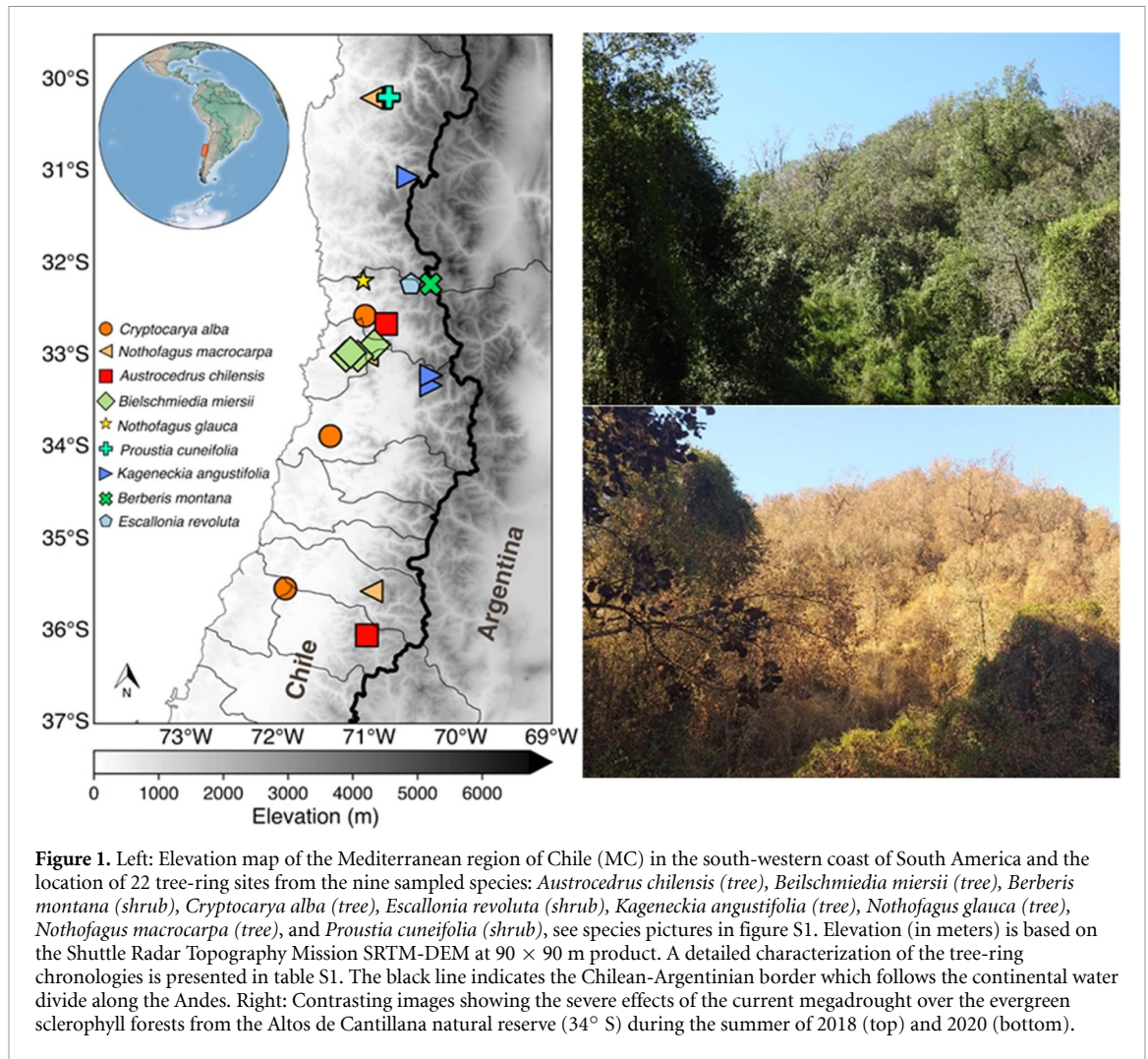
multi-century scales (Cherubini *et al* 2003, Villalba *et al* 2011). This enables the assessment of moisture variability's influence on tree growth and the reconstruction of past environmental conditions. Additionally, these environmental archives have been shown to be extremely useful for identifying patterns and changes in past hydroclimatic variability at different spatial and temporal scales in subtropical regions of both hemispheres (LeQuesne *et al* 2006, Christie *et al* 2011, Palmer *et al* 2015, Wilson *et al* 2016, Garreaud *et al* 2017, Cook *et al* 2020, Morales *et al* 2020, Williams *et al* 2020). Although tree-ring studies have assessed the connection between climate and tree growth (Venegas-González *et al* 2023), as well as precipitation and drought reconstructions in MC (LeQuesne *et al* 2006, Morales *et al* 2020), the role of soil moisture (SM) changes in relation to tree growth across multiple species and regional scale has yet to be investigated. Retrospective studies of MC hydroclimate and tree growth relations have primarily focused on the impact of low precipitation (LeQuesne *et al* 2006), rather than thoroughly assessing the effects of hydrological drought at surface and subsurface levels (Mishra and Singh 2010). Satellite-based SM data has proven a valuable tool in showcasing the significance of this parameter for tree growth and forest ecosystem dynamics (Muñoz *et al* 2014, Kostić *et al* 2021, Thomte *et al* 2022).

In this study, we establish a new tree-ring network spanning 22 sites across the MC region, encompassing 9 different species, including 3 new for tree-ring studies. The objectives of the present study are: (i) to evaluate the relationships between tree growth and SM both at local and regional scale across the network, (ii) to determine the common spatio-temporal tree growth patterns from the network and its relation with SM, and (iii) to utilize these registries to develop a SM reconstruction to evaluate the severity of the present megadrought within the context of the last 400 years. A deeper understanding of the relationship between multispecies tree growth and SM across the MC biome will enhance our knowledge of how this highly diverse and threatened ecosystem responds and adapts to ongoing and future climate changes in the MC region.

2. Methods

2.1. Study area

The MC region encompasses a strip of land between the Pacific coast and the central Andes of Chile



and Argentina (30° – 37° S), situated at the transition between the Atacama Desert in the north and the humid-temperate Andes in the south (figure 1). This area spans a latitudinal precipitation gradient from 100 to over 700 mm per year. The Mediterranean climate in the region exhibits a substantial oceanic effect that gradually diminishes from the coast towards the Andes, reaching up to ~ 7000 m a.s.l. only 200 km from the Pacific Ocean (Sarricolea et al 2017). Year-to-year precipitation variability is linked to the number of frontal systems arriving from the Pacific Ocean, highly influenced by variations in El Niño-Southern Oscillation (ENSO). ENSO, in turn, modulates the dynamics of the subtropical anticyclone (SPA) and the atmospheric pressure in the Amundsen-Bellinghausen sector of the South Pacific (Aceituno 1988, Montecinos and Aceituno 2003). During El Niño (La Niña) events, above-average (below-average) precipitation is expected in the MC during winter (Montecinos and Aceituno 2003). Several studies have linked high-latitude climatic forcing, such as the Southern Annular Mode (SAM, also known as the Antarctic Oscillation or AAO), to seasonal precipitation variability and its

long-term reduction trend in MC (Garreaud et al 2009, Quintana and Aceituno 2012, González-Reyes 2016, Boisier et al 2018). Currently, there has been a decrease in precipitation since the late 1970s as a result of climate changes caused by both natural and anthropogenic forcings (Boisier et al 2016, 2018, Villamayor et al 2022).

Several woody species were selected across the MC region to cover different environments within this biome, including the Andean mountains, the central valley, the coastal range, and the coastal lowlands. This encompasses sclerophyllous trees and shrubs, and deciduous forests (Gajardo 1994). We sampled 22 tree-ring sites from 9 species (figures 1, S1 and table S1). Three of these species have not been previously used for dendrochronological studies (*Escallonia revoluta*, *Berberis montana*, and *Nothofagus glauca*). Some of the sampling sites included transitional Andean zones (1400–2696 m.a.s.l.) with *Proustia cuneifolia* (Huañil) and *Berberis montana* (Michay) as arboreal shrubs, *Kageneckia angustifolia* (Frangel) as small trees, and the conifer *Austrocedrus chilensis* (Ciprés de la Cordillera). Tree-ring samples were collected from 2015 and 2021. Two to three cores were

extracted at breast height from trees using an increment borer, and cross-sections were obtained from multi-stemmed shrubs exhibiting eccentric growth patterns. Samples were air-dried in the laboratory and smooth-polished with sandpapers of decreasing grain size. The growth rings were dated following Schulman's convention for the Southern Hemisphere, which assigns to each ring the year when radial growth begins (Schulman 1956). Tree-ring widths were measured with a Velmex measuring system accurate to 0.001 mm. The accuracy of dating of the tree-ring series was verified using the COFECHA software (Holmes 1983). The dplR software package (Bunn 2008) was used to standardize the individual series of each site by fitting either a negative exponential curve or a straight line (Cook and Kairiukstis 2013). This technique effectively eliminates fluctuations caused by biological growth trends or other low-frequency variations not related to climate. The quality of each chronology was assessed using objective measures, including mean sensitivity (MS) to determine year-to-year variability within a ring-width series, first-order autocorrelation (AR1), mean series intercorrelation (RBAR), and the expressed population signal (EPS) which quantifies the degree to which the series portrays a hypothetically perfect chronology (Wigley *et al* 1984). Only periods in the chronologies with $EPS > 0.85$ were considered.

2.2. SM data

To evaluate the relationships between tree growth and SM, we used the data from by the Famine Early Warning Systems Network Land Data Assimilation System (FLDAS; McNally *et al* 2017). This global land surface model is driven by various datasets from satellite measurements and atmospheric analyses, which are evaluated using direct comparisons of outputs with independent measurements (ground/satellite) and indirect comparisons, including correlations of SM with vegetation indices (McNally *et al* 2017). The FLDAS data provides monthly gridded SM data at various depths, with a horizontal resolution of approximately 10 kilometers since the year 1982. The data is expressed as the volume of water per soil volume ($\text{m}^3 \text{m}^{-3}$). For our research, we focused on the SM layer between 0–10 centimeters depth.

2.3. Tree growth and SM relationships

Two methods were used to establish the connection between SM and tree-ring chronologies. First, we examined the connections at the individual chronology level, considering the SM grid at the chronology location. Additionally, we assessed these connections at a regional scale using the mean SM for the entire MC region (30° – 37° S, see figure 4(a)). The evaluations were conducted at the monthly scale over the common period 1982–2015, covered by the ring

width chronologies and the FLDAS. To identify the optimal correlation between SM and tree growth, we evaluated all possible monthly and seasonal combinations using Pearson correlation coefficients by running the KLIMA_trees routine (available at https://github.com/lonkotrewa/KLIMA_trees) in R project software (R; R Core Team 2020). Additionally, Monte Carlo bootstrap of 2000 simulations were performed to obtain robust Pearson correlations. We analyze the spatiotemporal patterns of radial growth for the nine species using the entire network of tree ring chronologies across the MC region (22 sites), using empirical orthogonal function (EOF) analyses (Wilks 2011). The EOF analysis accurately condenses the dominant growth patterns recorded in the 22 chronologies into a few series, referred as principal components (PCs). Our study primarily examines the first and second PCs (PC1 and PC2) and their associated spatial expression to characterize the dominant growth patterns. Finally, we determine the relationships between SM and the primary spatiotemporal pattern of MC tree growth by correlating the PC1 amplitudes with the SM mean from the entire MC region.

2.4. SM reconstruction

The hydrological year (May–April) SM reconstruction was generated by utilizing a principal component regression (PCR) method. This involved regressing the hydrological year SM (May–April) for the MC region against standard tree-ring chronologies, following the approach detailed by Cook *et al* (2007). Candidates predictors of SM were selected from tree-ring chronologies that began before 1950 and exhibited a significant correlation (p -value < 0.01) with hydrological year SM. These selected chronologies (see table S1) were then entered into a PCR to reduce the number of predictors and enhance the commonality present in the tree-ring records. Given the relative short SM record for calibration, the reconstruction model was developed using the 'leave-one-out' cross-validation procedure (Michaelsen 1987). In this approach each observation is successively withheld; a model is estimated on the remaining observations, and a prediction is made for the omitted observation. At the end of this procedure, the time series of predicted values assembled from the deleted observations is compared with the observed predictors to compute the validation statistics of model accuracy and error. The goodness of fit between observed and predicted SM values was tested based on the proportion of variance explained by the regression (R^2 -adj), the significance of the linear trend of the regression residuals evaluated by the Mann–Kendall test (Mann 1945, Kendall 1975), the reduction of error (RE) statistic over the verification period (Cook *et al* 1999), as well as the root-mean-square error (RMSE) statistic as a measure of inherent uncertainties in the reconstruction (Weisberg 1985).

To maximize the length of our tree-ring chronologies we utilized a nested PCR approach. This involved dropping shorter chronologies and repeating the PCR procedure using the remaining longer series (Meko 1997, Cook et al 2004). Calibration was performed on each nested PCR for the period 1982–2015. The final reconstruction was created by splicing the relevant segments from each full-period calibrated nested model. The mean and variance of each nested reconstruction were adjusted to those of the most replicated nest with the highest R^2 to prevent artificial changes in variance during the reconstruction caused by purely statistical, non-climatic factors (Cook et al 2004, Wilson et al 2007). To minimize potential underestimation of extreme hydrological year regional SM values during the reconstruction, we restored the lost variance by rescaling the final reconstruction to match the variance of the observed SM data during the calibration period (Cook et al 2004). After that, we updated the final nested reconstruction, covering the period 1616–2018, with FLDAS regional data until 2021.

2.5. Climate forcings and MC SM variability

To determine the main relationships between MC SM variability and large-scale climate, we performed multiple regression analyses using several climate indices as potential predictors of the MC SM record. These climate indices (see table 1) have been widely used to characterize climatic conditions in South Western South America and were thus possibly linked to interannual SM variability across MC. As some of these candidate predictors may not be statistically independent, a stepwise regression approach (F-to-enter 0.05, F-to-remove 0.10) was used to avoid multicollinearity among the predictors and develop a reliable regression model. Since most of the seasonal climatic index series exhibit strong serial correlations, we utilized the prewhitened versions of the seasonal climatic indices as predictors of the prewhitened SM record. Additionally, we estimated the spatial correlation pattern between the reconstructed hydrological year SM and the mean annual sea level pressure (SLP) (May–April; 0.25×0.25 gridded cell) from the ERA5 reanalysis (Hersbach et al 2020).

3. Results

3.1. Tree growth and SM relationships

Twenty-two tree-ring sites were analyzed to assess the link between tree growth and SM variability at both local and regional scales, utilizing FLDAS SM data spanning the period 1982–2015. The results reveal a generally strong and positive relationship between tree growth and May–April SM at both local (tree-ring site vs. respective SM grid) and regional (tree-ring site vs. entire MC region) scales, as illustrated in figure 2. Significant positive correlations were recorded at both

local and regional scales for most sites, with stronger relationships identified at the local scale (figure 2). The highest correlation coefficients were observed for *K. angustifolia* (PYL) at both local and regional scales, *C. alba* (PLC) and *N. macrocarpa* (ACH) at the local scale, and *B. miersii* (BLC) and *K. angustifolia* (MET) at the regional scale. Several *C. alba* sites displayed significant correlations with both *in-situ* and regional May–April mean SM values in the MC. Similarly, a majority of *B. miersii* chronologies exhibited strong relationships with SM values ($r > 0.55$). Furthermore, the three species *E. revoluta* (SOB), *N. glauca* (HPL), *B. montana* (PAR), utilized for the first time in tree-ring studies, demonstrated significant correlations with May–April mean SM at local and regional scales, demonstrating their utility for dendrochronological studies.

3.2. Spatiotemporal patterns of tree growth

Utilizing 22 ring-width chronologies from nine species of shrubs and trees distributed throughout the MC region, the first two PCs explain 37% of the total variance in tree growth over the period 1970–2015 (figure 3). The first principal component (PC1) accounts for 27% of the total variability, indicating a significant contribution from the entire tree ring network located between 32° and 34° S (figure 3(a)). Several species chronologies, including those from *B. miersii*, *C. alba*, and *K. angustifolia* exhibit high PC1 loadings (figure 3(a)). PC1 amplitudes above the average prevail during the intervals of 1977–1984, 1990–1992, and 2000–2006. In contrast, years below the mean are recorded during the intervals of 1988–1990, 1994–1999, and the extended period of low growth between 2007–2015, as illustrated in figure 3(b). The PC2 accounts for 10% of the total variance, with a significant contribution from the *P. cuneifolia* and *N. macrocarpa* chronologies situated at the northern boundary of the MC region ($\sim 30^\circ$ S; figure 3(c)). Temporal variations in PC2 reveal above-average tree growth intervals primarily from 1971 to 1976 and 1987 to 1991, while below-average periods were identified mainly from 1977 to 1979, 1983 to 1988 and 1997 to 2003 (figure 3(d)). Additionally, a remarkable interannual growth variability has been observed since 2004.

3.3. Regional pattern of tree growth and SM relationships

We examined the correlation between temporal changes in PC1 and the gridded mean May–April SM in the MC region from 1982 to 2015 using Pearson correlation coefficients. The May to April intervals were selected due to the high significant correlations obtained during these months (figure S2), and also not observed in another climatic variables such as May–April precipitation and mean air temperature during the same months (figure S3). We found strong

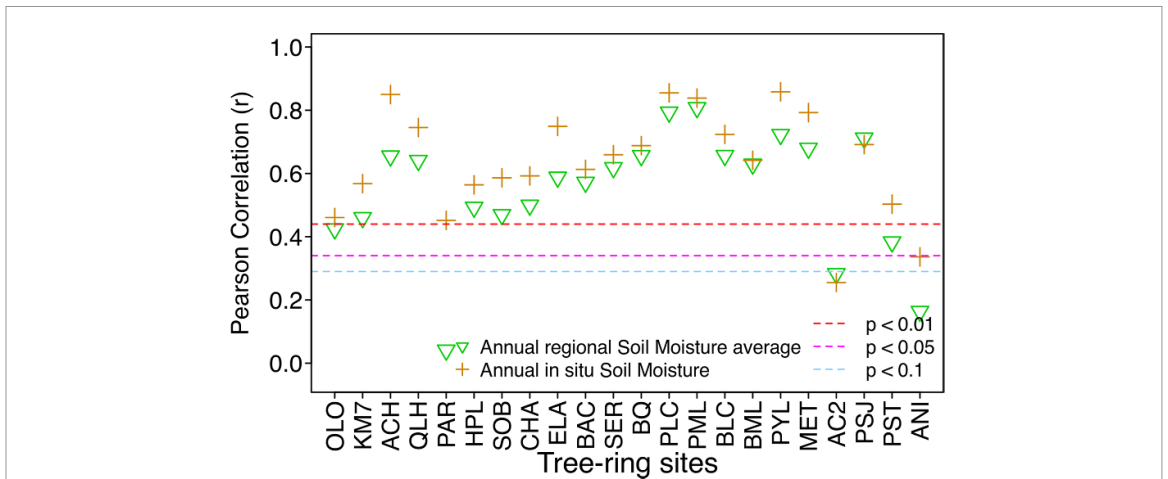


Figure 2. Pearson correlation coefficients between each from the 22 tree-ring width chronology from nine species and 10 × 10 km gridded monthly averaged during hydrological year (May–April) FLDAS soil moisture (SM) at local (SM grid corresponding to chronology location) and regional (Mediterranean Chile region see figure 4(a)) scales for the 1982–2015 period. In both cases, the Pearson correlation coefficients were calculated using 2000 bootstrap simulations. Chronologies are ordered from north (left) to south (right) latitudinal gradient and details about species, locations and specific statistics are indicated in table S1.

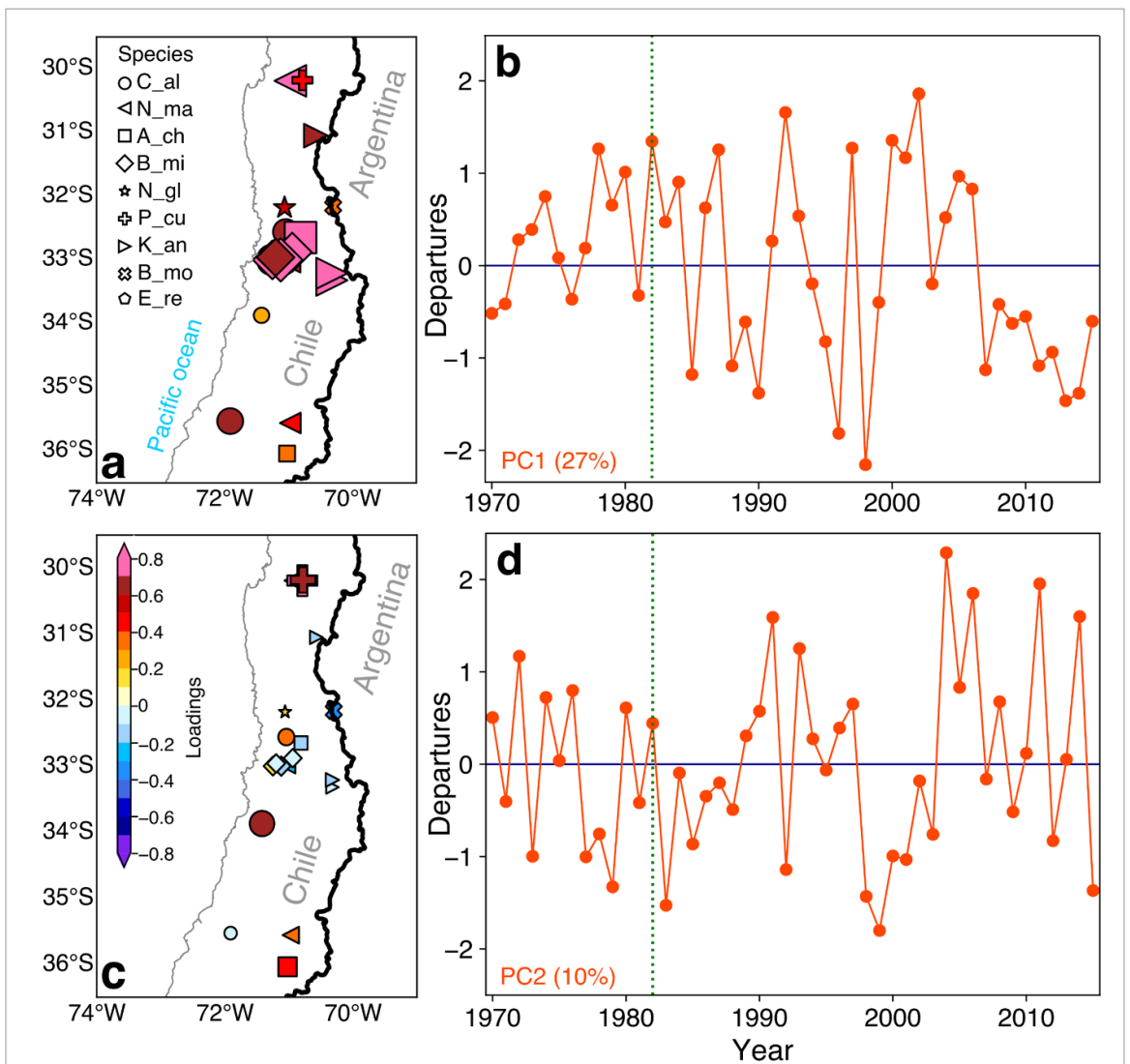


Figure 3. Main spatio-temporal -growth patterns of the 22 tree-ring chronologies from nine woody species. The (a) and (c) panels correspond to the spatial loadings of the leading two empirical orthogonal function (EOF) modes for the 22 tree-ring chronologies (the size of the symbols is in accordance with the value of the loading). Time series of the corresponding leading modes (PC1 and PC2) explaining 27% and 10% of the variance of the entire tree-ring network during the 1970–2015 common period.

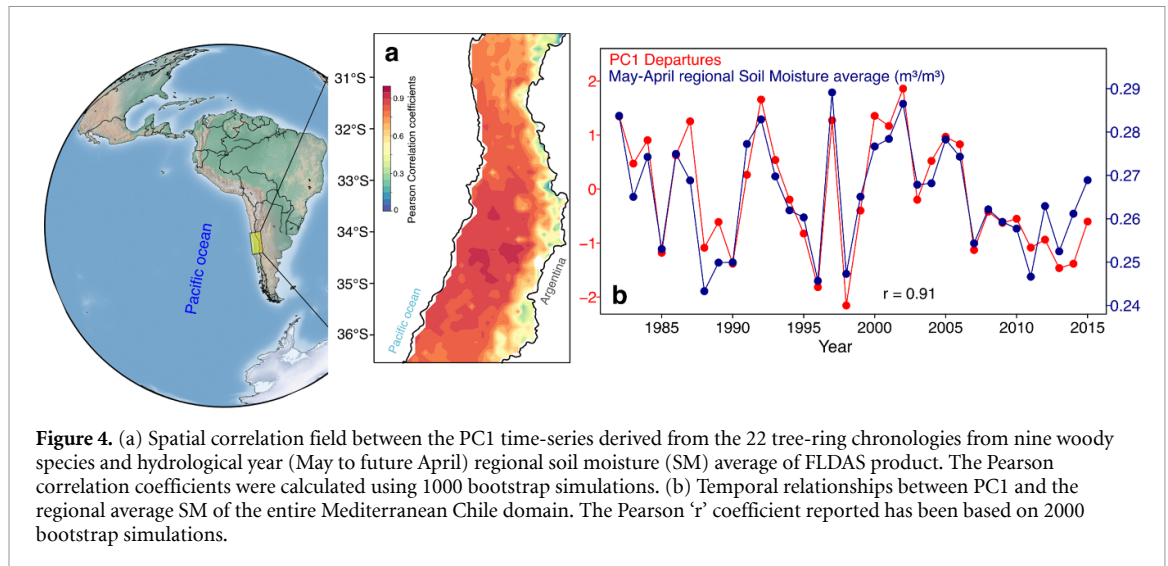


Figure 4. (a) Spatial correlation field between the PC1 time-series derived from the 22 tree-ring chronologies from nine woody species and hydrological year (May to future April) regional soil moisture (SM) average of FLDAS product. The Pearson correlation coefficients were calculated using 1000 bootstrap simulations. (b) Temporal relationships between PC1 and the regional average SM of the entire Mediterranean Chile domain. The Pearson 'r' coefficient reported has been based on 2000 bootstrap simulations.

spatial correlations between PC1 and the annual variability of SM, particularly in the 33°–36° S region, where Pearson correlation coefficients were notably high and significant ($r > 0.8$; figure 4(a)). In temporal terms, both time series exhibit synchronicity during several years, displaying consistently low values of yearly regional SM starting from 2007 (figure 4(b)). Furthermore, a robust correlation ($r = 0.91$) was recorded between SM and the first PC of the radial growth patterns for the nine different species in the MC from 1982 to 2015. We also identified that correlations between the PC1 and May–April SM are highest compared to ERA5 Precipitation and mean air temperature during May–April (figure S3).

3.4. Reconstruction of SM in mediterranean Chile

The robust correlation between PC1 and SM content in the MC region during May to April months ($r = 0.91$, 1982–2015; figure 4) represents a novel finding not previously reported in tree-ring studies conducted in South America. Building upon this significant result, we conducted a nested May to April SM reconstruction spanning the last four centuries (1616–2018) to characterize the temporal variability and changes in SM in the MC region. To include the years 2019 to 2021, we included actual FLDAS measurements into the reconstructed series. Our May–April regional SM reconstruction is based on seventeen chronologies from various tree and shrub species. These species exhibit a significant correlation (p -value < 0.01) with May–April SM content at both local and regional scales within the MC region (figure 2). We only selected tree and shrub chronologies with an EPS greater than 0.85 since 1950. Our new findings demonstrate the robustness of our reconstruction and its significant correlation with observed May–April SM variations from 1982 to 2015 ($r = 0.91$; figure 5(a)). Additionally, the RMSE values were low, and there is not any significant

trend in the residuals of the regression models (table S2). The final nested reconstruction effectively reproduced total variance values between 0.43 and 0.81 (figure 5(c)). For a complete summary of the reconstructions, as well as their corresponding statistics and intervals needed to generate the final nested reconstruction, refer to table S2. Since several chronologies contain information beyond 2015 (table S1), we perform reconstructions up to 2018 using the PC reconstruction. The SM reconstruction displays extended periods of low and high May–April SM values from 1616 AD to the present day. For example, there were periods of exceptionally high values found during 1650–1675, 1725–1750, 1820–1860, 1890–1910, and 1960–1990 (figure 5(b)). Conversely, intervals of low SM values were observed during 1680, 1751–1770, 1790–1820, 1911–1950, and since 2007 onwards.

3.5. Climate forcings and MC SM variability

The multivariate stepwise regression trials revealed that, except the latitudinal position of the Southern Pacific anticyclone (SPAL), all climatic indices for December to February (austral summer) exhibit consistent and significant relationships with the observed regional May–April SM derived from FLDAS product from 1983 to 2021 (table 1). During autumn (March to May; MAM), significant relationships present only significant values with the intensity of the Southern Pacific anticyclone (SPAI). Significant correlations were also detected during winter (June to August; JJA). Significant relationships were found with Niño 3.4, SOI, and the TPI, with the strongest correlation observed with the SPAI. In winter, utilizing the full range of climate indices, the model was able to replicate 33% of the overall variance. On an annual scale, the stepwise regression model was able to replicate 31% of the total variability, where the SOI and SPAI was the most relevant climate

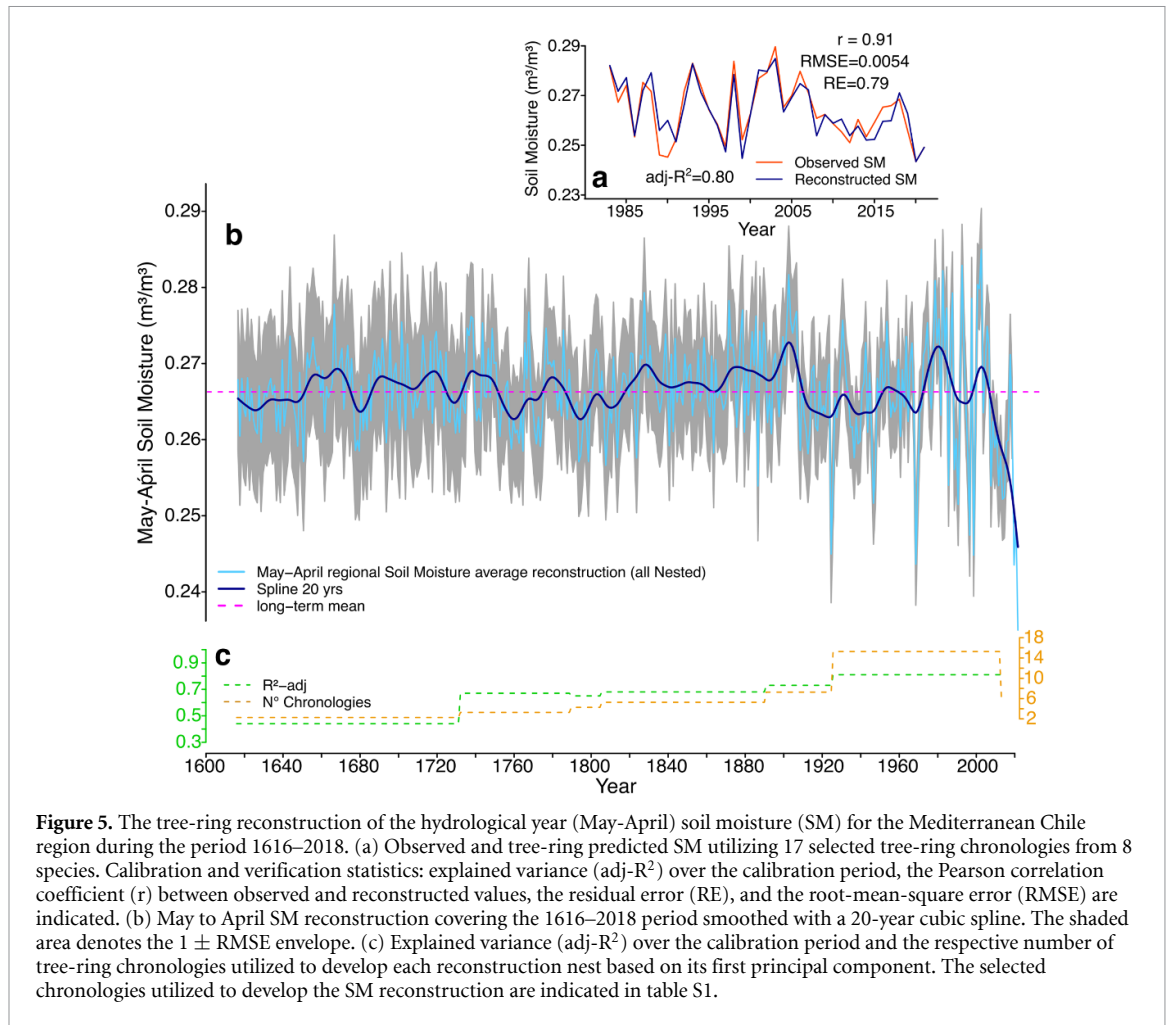


Figure 5. The tree-ring reconstruction of the hydrological year (May–April) soil moisture (SM) for the Mediterranean Chile region during the period 1616–2018. (a) Observed and tree-ring predicted SM utilizing 17 selected tree-ring chronologies from 8 species. Calibration and verification statistics: explained variance (adj-R^2) over the calibration period, the Pearson correlation coefficient (r) between observed and reconstructed values, the residual error (RE), and the root-mean-square error (RMSE) are indicated. (b) May to April SM reconstruction covering the 1616–2018 period smoothed with a 20-year cubic spline. The shaded area denotes the $1 \pm \text{RMSE}$ envelope. (c) Explained variance (adj-R^2) over the calibration period and the respective number of tree-ring chronologies utilized to develop each reconstruction nest based on its first principal component. The selected chronologies utilized to develop the SM reconstruction are indicated in table S1.

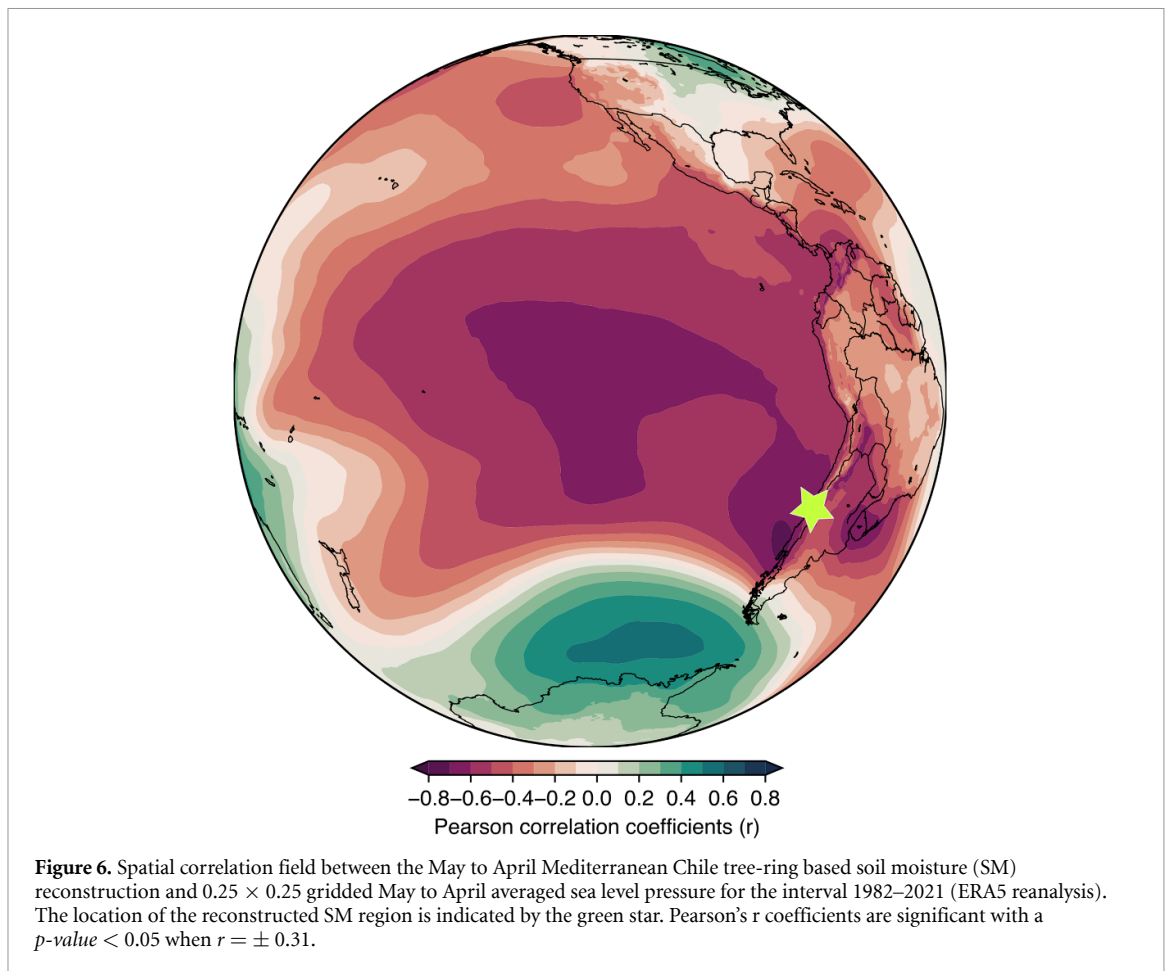
Table 1. Multivariate regression trials between 1983–2021 prewhitened versions of the observed May to April soil moisture average for MC and seasonally averaged estimates for the six climatic indices. Four 3-month seasons starting in May of the previous year were used to current April, and candidate predictors were selected following a stepwise regression approach (F-to-enter 0.05, F-to-remove 0.10). The r denotes the correlation coefficient between the observed May to April soil moisture average for MC and seasonal averages for each climatic index; Beta denotes the standardized regression coefficients used to compare the relative strength of the various predictors within each model; Adj R^2 denotes the coefficient of determination adjusted for the number of predictors in the model, and # indicates that none of the predictors passed the threshold value for F-to-enter. The climate indices acronyms mean N3.4: SST anomalies for the Niño3.4 region (Trenberth 1997), SOI: Southern Oscillation Index (Ropelewski and Jones 1987), TPI-IPO: Interdecadal Pacific Oscillation (Henley et al 2015), SAM: Southern Annular Mode (Marshall 2003), SPAI: Intensity of the South Pacific Subtropical Anticyclone, and SPAL: latitudinal position of the South Pacific Subtropical Anticyclone. Both indexes based on Barrett and Hameed (2017). For the respective references see Methods section 2.4.

Climate Indices	DJF (summer) r (Beta)	MAM (autumn)	JJA (winter)	SON (spring)	Annual
N3.4	0.42** (−0.35)	0.09 (−0.54)	0.48** (0.10)	0.48 (0.18)	0.47** (−0.09)
SOI	−0.48** (0.12)	−0.22 (−0.12)	−0.51** (−0.20)	−0.40 (0.15)	−0.54*** (−0.28)
TPI IPO	0.49** (0.73)	0.18 (0.49)	0.48** (−0.01)	0.49*** (0.47)	0.52** (0.20)
SAM	−0.33* (−0.17)	−0.08 (−0.01)	0.09 (0.03)	−0.08 (0.06)	−0.20 (−0.05)
SPAI	−0.30* (0.10)	−0.38* (−0.36)	−0.53** (−0.41)	−0.40* (−0.04)	−0.54*** (−0.20)
SPAL	0.01 (0.17)	0.21 (−0.04)	0.01 (−0.10)	0.28 (0.30)*	0.16 (0.09)
Adj R^2	0.28	0.12	0.33	0.31	0.31

(* p -value < 0.05, ** p -value < 0.01, *** p -value < 0.001).

index predictors (table 1). At a geographic level, the reconstruction of SM and the mean SLP field during May to April, which was obtained from the ERA5 reanalysis (Hersbach et al 2020), show substantial negative correlations, primarily over the Tropical and

mid-latitudes of the Pacific Ocean (figure 6). Positive correlations are observed at high latitudes over the Amundsen Sea low domain, demonstrating the role of circum-Antarctic blocking centers on MC hydro-climate variability.



4. Discussion

4.1. Tree-growth and SM relationships

Interannual variations in radial growth of nine tree and shrub species at 22 sites in the MC (30° – 37° S) region are closely related to variations in May to April SM (0–10 cm depth), derived from FLDAS observations over the period 1982–2015. In addition, a previous study developed by Thomte *et al* (2022), has used this product to assess the relationship between tree growth and SM levels for *Pinus kesiya* in the southern Himalayas, indicating the utility of this product in tree-ring analyses.

We used three new species for dendrochronological studies (*B. montana*, *E. revoluta*, and *N. glauca*), thus increasing the number of species that compose the current South American network of dendrochronological records (Boninsegna *et al* 2009, Morales *et al* 2020). Our correlations results show that the relationships between tree and shrub chronologies and May to April SM are exceptionally strong, demonstrating the high dependence between vegetation growth and SM along the MC region. These positive relationships are remarkable at both local (chronology site) and regional scales using mean May to April SM across the MC. Our results show that the nine study species are sensitive to SM variations across the MC region. *C. Alba* (PLC and PML sites;

figure 2) show the highest correlation values among the other species used in this study.

Our reconstruction demonstrates the exceptional nature of the present MC megadrought within the context of the last 400 years. Recent studies have reported the severe growth decline in several plant species in the MC as a result of the current unprecedented megadrought during the last decade (Garreaud *et al* 2017, Miranda *et al* 2020, 2023, Venegas-González *et al* 2018, 2023). These plant species and probably many others from the MC region, have confronted extreme climate and environmental conditions due to the persistent severe aridity conditions after 2010 (Garreaud *et al* 2020, Matskovsky *et al* 2021, Venegas-González *et al* 2023). The propagation of this megadrought through the water cycle has led to a substantial decline in snowpack, glacier area and streamflow with the subsequent negative effects in water availability across Central Chile (Cordero *et al* 2019, Masiokas *et al* 2019, Ayala *et al* 2020, Muñoz *et al* 2020, Garreaud *et al* 2020, Alvarez-Garretón *et al* 2021), triggering unfavorable consequences for the Mediterranean forests in Central Chile (Miranda *et al* 2023). This biome provides a variety of fundamental ecosystem services to the society (Gajardo-Rojas *et al* 2022, Smith-Ramírez *et al* 2023), and have been proposed as a key element to implement nature based solutions for water security for the region

(Schneider-Valenzuela *et al* 2023). These pervasive drought conditions in MC are well reflected in the SM changes during the last decade, representing the most severe hydroclimatic change in Mediterranean ecosystems worldwide, with profound effects on forest ecosystems (Miranda *et al* 2023). Conservation efforts are crucial to protect and preserve the remaining MC forests to maintain their resilience capacity and provide mitigation measures at the local level during future climate.

In spatial terms, we record that tree-ring sites located between 32°–34° S present the highest loadings factors values within the PCA analysis, being particularly relevant the decline of growth patterns from around the year 2007 onwards exhibited by the first dominant pattern of radial growth in both trees and shrubs. Several sampling sites of *B. miersii* and *C. alba* are located at these latitudes in Central Chile, where we registered the strongest relationship with MC SM variability and changes. The first and second temporal growth patterns exhibit contrasting patterns. We also identified a decline in growth in the PC2 pattern but since 2004 and with a marked interannual variability. This behavior aligns with the hydroclimate variability toward the northern sector of the MC region at the transition with the Atacama Desert (Garreaud *et al* 2009, González-Reyes *et al* 2017). The year showing the most severe reduction in growth over the 1982–2015 interval was during the strong 1998 La Niña event, following the strong 1997 El Niño event. Our results also indicate a persistent and severe decline in radial growth across the MC region around the year 2007 onwards depicted by the PC1, in parallel to the SM reduction indicated by the FLDAS dataset. The strong decline around the year 2007 aligns with the regional megadrought identified by Garreaud *et al* (2017), it initiates several years earlier. This may suggest that SM and tree-growth in MC recorded aridity changes beyond precipitation scarcity, integrating the combined effect of precipitation reductions and the increment of heatwaves and extreme temperatures during the last decades (González-Reyes *et al* 2023). This suggests that environmental and aridity changes in the MC region started around the year 2007, preceding the marked precipitation reduction in 2010, and today stand up as the most severe drought between Mediterranean ecosystems worldwide (Miranda *et al* 2023). Our findings also indicate that SM is the main factor controlling plant growth patterns at the regional scale in the MC region, and is the main forcing behind the so-called MC forest decline (Miranda *et al* 2020, 2023, Venegas-González *et al* 2023).

Heatwaves severely affect SM during the spring-summer growing season in MC (González-Reyes *et al* 2023). This could be amplified during drought episodes such as the current megadrought in Central Chile. Recent studies have addressed the role of

droughts in amplifying the effects of heatwaves, leading to severe SM decline (Miralles *et al* 2014). A study conducted by Piticar (2018) using weather stations across MC identified an increase in heatwaves during the period 1961–2016. Using a high-resolution maximum temperature gridded, González-Reyes *et al* (2023) reported similar results. The severe forests-browning (Miranda *et al* 2020, 2023) and tree-growth decline (Venegas-González *et al* 2023 and this work), could be related to the combined effect of the moisture decline reported in the present study, the precipitation decline during the megadrought (Garreaud *et al* 2017), and the regional increase in heatwaves in the MC region (González-Reyes *et al* 2023).

4.2. Four hundred years SM dynamics and changes

Our results indicate that the recent multispecies tree-growth decline reveals a severe and unprecedented aridity change in Mediterranean Chile within the context of the last 400 years. The developed SM reconstruction represents the first of its type in South America and records several low and high multi-decadal intervals from 1616 to the present in the MC region (figure 5). These periods are also identified in other MC hydroclimate reconstructions, such as the South American Drought Atlas (SADA; Morales *et al* 2020), from which our SM reconstruction is almost totally independent, sharing just one of our seventeen chronologies utilized as predictors. In addition, the PC1 nests exhibit a robust spatial pattern in terms of Pearson correlations with SADA during the 1928–2000 (figure S5). On the other hand, the remarkable relationship between SM and MC woody species growth indicates the high vulnerability of MC forest ecosystem dynamics to SM variations and changes. Based on these relationships, the present SM reconstruction reproduces by far the highest observed amount of variance compared to any hydroclimate reconstruction in South America (i.e. LeQuesne *et al* 2006, LeQuesne *et al* 2009, Christie *et al* 2011, Muñoz *et al* 2020, Hadad *et al* 2021).

The regional MC May–April SM reconstruction presents a strong negative correlation with the mean annual intensity of the Southern Pacific Anticyclone (SPA; table 1, figure 6). The reconstruction shows a close relationship with the intensity of pressure fields across the Pacific Ocean, particularly at the Southern Hemisphere mid-latitudes where the SPA is located, indicating the key role of this forcing on SM dynamics in the MC region. Conversely, positive and significant correlation values are identified along the Austral Ocean, specifically over the Amundsen–Bellingshausen Sea. Over this circum-Antarctic region, variations in the intensity of the low-pressure system called Amundsen Sea Low occur (Hosking *et al* 2016), playing a key role as a blocking center of the storm tracks at higher latitudes favoring

the incursion of wet air masses at the MC latitudes. Precipitation in MC is mostly a result of frontal passages and moisture advection associated with mid-latitude cyclones, therefore weaker SPAI allow for greater precipitation (Barrett and Hameed 2017). The strong negative (positive) correlations between MC SM and SLP all across the mid- (high-) latitudes highlights the previous relation (figure 6), demonstrating the key role of SPAI allowing the passage of storm tracks over MC. In addition, significant and an inverse relationship between the SPAI developed by Barrett and Hameed (2017) and our SM reconstruction are also recorded during the 1982–2021 period (figure S6).

ENSO also plays a role on MC SM variations, with the Southern Oscillation Index (SOI) correlating during winter SM and the N3.4. region sea surface temperatures (SST) during summer. During El Niño (La Niña) years, an enhanced (decreased) subtropical moisture transport leads to larger values of precipitable water and heightened zonal integrated water vapor transport, resulting in greater (lesser) precipitation in MC (Campos and Rondanelli 2023). Spatial correlations between the regional May–April SM reconstruction and SST show positive correlations in the tropical Pacific, particularly toward the subtropical east in front of the Chilean coast, and in the Amundsen–Bellingshausen Sea in the Austral Ocean (figure S7). During spring–summer, the interdecadal Pacific Oscillation (TPI–IPO index) also plays a relevant role in the variability of MC SM (table 1). In addition, the decadal to multidecadal variability highlighted in our reconstruction is likely influenced by IPO variability (figure S8). The strong negative correlations of MC SM with SLP over the subtropical Pacific Ocean and the SPAI variability are mainly determined by the subsiding branch of the Hadley Cell in the Southern Hemisphere (Fahad et al 2020, Flores–Aqueveque et al 2020, Villamayor et al 2022). These correlations are in concordance with the expected influence of this circulation pattern over the subtropics (Nguyen et al 2013, 2015, figure 3). The descending branch of the Hadley Cell can be considered the ‘edge of the tropics’, and determines the subtropical high–pressure belt, influencing the latitudinal distributions of precipitation, clouds cover, relative humidity, and drought severity of the subtropical region where MC is located. Over the last four decades the Hadley Cell has been expanding poleward, contributing to increased droughts over many subtropical regions (Lucas et al 2012). This expansion has been attributed to a combination of natural and anthropogenic climate forcings, with increasing greenhouse gasses concentrations and ozone depletion over Antarctica playing a key role (Nguyen et al 2015, Waugh et al 2015). Presently, anthropogenic forcing appears as one of the leading factors of precipitation and aridity change in MC (Boisier et al 2016, 2018).

5. Conclusions

We determined the relationships between May–April SM content derived from the FLDAS global model and radial growth of nine woody species distributed in 22 sampling sites across Mediterranean Chile. Three of these species have been used for the first time in ring-width studies (*B. montana*, *E. revoluta*, and *N. glauca*). Chronologies from several tree species, such as *B. miersii* and *C. alba*, reveal a strong relationship with SM variations during the period 1982–2015 ($r > 0.80$). The first mode of interannual variability in radial growth from the tree-ring network shows a remarkable correlation of 0.91 with soil water content, demonstrating the vulnerability of these species to changes in SM across the MC region.

The ring-width-based SM reconstruction shows a severe SM decline from around the year 2007, revealing a recent unprecedented regional aridity change within the context of the past four centuries. The increase in the pressure intensity of the South Pacific Subtropical Anticyclone appears as the main large-scale forcing instigating the present aridity conditions in MC. Our results are in agreement with previous studies indicating that MC is suffering the worst persistent drought of the last centuries (Garreaud et al 2017, Cook et al 2022). The present browning and forest decline in Central Chile stands out as the most severe of its type among Mediterranean ecosystems worldwide (Miranda et al 2023), posing enormous challenges for the management and conservation of this global biodiversity hotspot. The last decade mean regional precipitation of MC is similar to the expected regional precipitation amount for the period 2070–2090 under RCP8.5 scenario (Boisier et al 2018). Detailed assessments of MC future SM variability would be relevant to forecast the potential effects of climate change over the threatened forest ecosystems of Central Chile.

Data availability statement

The data that support the findings of this study are openly available at the following URL/DOI: <https://zenodo.org/records/10687704>.

Acknowledgments

This work was supported by the National Agency for Research and Development Chile (ANID/PAI/77190101, ANID/Subdirección de Capital Humano/Doctorado Nacional 2024/21241735, ANID/Fortalecimiento Centros Regionales/CERES/R23F0003. FONDECYT projects 1221307, 1201411, 1221701, 1201714, 11230437, 1241699, 1241971, FONDAP 1523A0002, FONDAP 15150003 and BASALFB210018). We thank Arón

Cádiz for graciously providing photographs of several species, as well as the landowners and the Chilean Forest Service CONAF for granting permission to collect the tree-ring samples. Finally, we thank the three anonymous reviewers for their many insightful comments and suggestions to improve our article.

ORCID iDs

Álvaro González-Reyes  <https://orcid.org/0000-0001-7525-349X>

Duncan A Christie  <https://orcid.org/0000-0003-2540-0986>

Isadora Schneider-Valenzuela  <https://orcid.org/0000-0002-2047-4153>

Alejandro Venegas-González  <https://orcid.org/0000-0003-4568-4533>

Ariel A Muñoz  <https://orcid.org/0000-0002-1719-4900>

Martin Hadad  <https://orcid.org/0000-0002-9334-064X>

Tania Gipoulou-Zuñiga  <https://orcid.org/0009-0002-3101-7203>

Stephanie Gibson-Carpintero  <https://orcid.org/0000-0002-9036-8823>

Luiz Santini-Junior  <https://orcid.org/0000-0002-5414-5921>

Carlos LeQuesne  <https://orcid.org/0000-0001-7124-0683>

Ricardo Villalba  <https://orcid.org/0000-0001-8183-0310>

References

- Aceituno P 1988 On the functioning of the southern oscillation in the south american sector. Part I: surface climate *Mon. Weather Rev.* **116** 505–24
- Allen C D, Breshears D D and Mcdowell N G 2015 On underestimation of global vulnerability to tree mortality and forest die-off from hotter drought in the Anthropocene *Ecosphere* **6** 1–55
- Alvarez-Garretón C, Boisier J P, Garreaud R, Seibert J and Vis M 2021 Progressive water deficits during multiyear droughts in basins with long hydrological memory in Chile *Hydrol. Earth Syst. Sci.* **25** 429–46
- Anderegg W R L et al 2015 Tree mortality from drought, insects, and their interactions in a changing climate *New Phytol.* **208** 674–83
- Ayala Á, Fariás-Barahona D, Huss M, Pellicciotti F, McPhee J and Farinotti D 2020 Glacier runoff variations since 1955 in the Maipo River basin, in the semiarid Andes of central Chile *The Cryosphere* **14** 2005–27
- Barrett B S and Hameed S 2017 Seasonal variability in precipitation in central and Southern Chile: modulation by the South Pacific high *J. Clim.* **30** 55–69
- Boisier J P, Alvarez-Garretón C, Cordero R R, Damiani A, Gallardo L, Garreaud R D, Lambert F, Ramallo C, Rojas M and Rondanelli R 2018 Anthropogenic drying in central-southern Chile evidenced by long-term observations and climate model simulations *Elementa* **6** 74
- Boisier J P, Rondanelli R, Garreaud R D and Muñoz F 2016 Anthropogenic and natural contributions to the Southeast Pacific precipitation decline and recent megadrought in central Chile *Geophys. Res. Lett.* **43** 413–21
- Boninsegna J A et al 2009 Dendroclimatological reconstructions in South America: a review *Palaeogeogr. Palaeoclimatol. Palaeoecol.* **281** 210–28
- Bowman D M J S, Kolden C A, Abatzoglou J T, Johnston F H, van der Werf G R and Flannigan M 2020 Vegetation fires in the Anthropocene *Nat. Rev. Earth Environ.* **1** 10
- Bunn A G 2008 A dendrochronology program library in R (dplR) *Dendrochronologia* **26** 115–24
- Burger F, Brock B and Montecinos A 2018 Seasonal and elevational contrasts in temperature trends in Central Chile between 1979 and 2015 *Glob. Planet. Change* **162** 136–47
- Campos D and Rondanelli R 2023 ENSO-related precipitation variability in Central Chile: the role of large scale moisture transport *J. Geophys. Res. Atmos.* **128** e2023JD038671
- Cerda R, Deheuvels O, Calvache D, Niehaus L, Saenz Y, Kent J, Vilchez S, Villota A, Martínez C and Somarrriba E 2014 Contribution of cocoa agroforestry systems to family income and domestic consumption: looking toward intensification *Agrofor. Syst.* **88** 957–81
- Cherubini P, Gartner B L, Tognetti R, Bräker O U, Schoch W and Innes J L 2003 Identification, measurement and interpretation of tree rings in woody species from mediterranean climates *Biol. Rev. Camb. Phil. Soc.* **78** 119–48
- Christie D A, Boninsegna J A, Cleaveland M K, Lara A, Le Quesne C, Morales M S, Mudelsee M, Stahle D W and Villalba R 2011 Aridity changes in the temperate-mediterranean transition of the Andes since ad 1346 reconstructed from tree-rings *Clim. Dyn.* **36** 1505–21
- Cook B I et al 2022 Megadroughts in the common Era and the Anthropocene *Nat. Rev. Earth Environ.* **3** 741–757
- Cook E R et al 2020 The European Russia drought Atlas (1400–2016 CE) *Clim. Dyn.* **54** 2317–35
- Cook E R and Kairiukstis L A 2013 *Methods of Dendrochronology: Applications in the Environmental Sciences* (Springer)
- Cook E R, Meko D M, Stahle D W and Cleaveland M K 1999 Drought reconstructions for the Continental United States *J. Clim.* **12** 1145–62
- Cook E R, Seager R, Cane M A and Stahle D W 2007 North American drought: reconstructions, causes, and consequences *Earth Sci. Rev.* **81** 93–134
- Cook E R, Woodhouse C A, Eakin C M, Meko D M and Stahle D W 2004 Long-term aridity changes in the Western United States *Science* **306** 1015–8
- Cordero R R, Asencio V, Feron S, Damiani A, Llanillo P J, Sepulveda E, Jorquera J, Carrasco J and Casassa G 2019 Dry-season snow cover losses in the Andes (18°–40°S) driven by changes in large-scale climate modes *Sci. Rep.* **9** 16945
- Fahad A A, Burls N J and Strasberg Z 2020 How will southern hemisphere subtropical anticyclones respond to global warming? Mechanisms and seasonality in CMIP5 and CMIP6 model projections *Clim. Dyn.* **55** 703–18
- Flores-Aqueveque V, Rojas M, Aguirre C, Arias P A and González C 2020 South Pacific Subtropical high from the late Holocene to the end of the 21st century: insights from climate proxies and general circulation models *Clim. Past* **16** 79–99
- Forzieri G, Dakos V, McDowell N G, Ramdane A and Cescatti A 2022 Emerging signals of declining forest resilience under climate change *Nature* **608** 7923
- Fuentes-Castillo T 2020 Hotspots and ecoregion vulnerability driven by climate change velocity in Southern South America *Reg. Environ. Change* **20** 27
- Fuentes-Castillo T, Scherson R A, Marquet P A, Fajardo J, Corcoran D, Román M J and Plissock P 2019 Modelling the current and future biodiversity distribution in the Chilean Mediterranean hotspot. The role of protected areas network in a warmer future *Divers. Distrib.* **25** 1897–909
- Gajardo R 1994 *La vegetación natural de Chile: Clasificación y distribución geográfica* (Editorial Universitaria) 1a.ed
- Gajardo-Rojas M, Muñoz A A, Barichivich J, Klock-Barría K, Gayo E M, Fontúrbel F E, Olea M, Lucas C M and Veas C

- 2022 Declining honey production and beekeeper adaptation to climate change in Chile *Prog. Phys. Geogr.: Earth Environ.* **46** 737–56
- Garreaud R D, Alvarez-Garreton C, Barichivich J, Boisier J P, Christie D, Galleguillos M, LeQuesne C, McPhee J and Zambrano-Bigiarini M 2017 The 2010–2015 megadrought in central Chile: impacts on regional hydroclimate and vegetation *Hydrol. Earth Syst. Sci.* **21** 6307–27
- Garreaud R D, Boisier J P, Rondanelli R, Montecinos A, Sepulveda H H and Veloso-Aguila D 2020 The central Chile mega drought (2010–2018): a climate dynamics perspective *Int. J. Climatol.* **40** 421–39
- Garreaud R D, Vuille M, Compagnucci R and Marengo J 2009 Present-day South American climate *Palaeogeogr. Palaeoclimatol. Palaeoecol.* **281** 180–95
- González-Reyes Á 2016 Ocurrencia de eventos de sequías en la ciudad de Santiago de Chile desde mediados del siglo XIX *Rev. Geogr. Norte Gd.* **64** 21–32
- González-Reyes Á, Jacques-Coper M, Bravo C, Rojas M and Garreaud R 2023 Evolution of heatwaves in Chile since 1980 *Weather Clim. Extremes* **41** 100588
- González-Reyes Á, McPhee J, Christie D A, Le Quesne C, Szejner P, Masiokas M H, Villalba R, Muñoz A A and Crespo S 2017 Spatiotemporal variations in hydroclimate across the Mediterranean Andes (30°–37°S) since the early twentieth century *J. Hydrometeorol.* **18** 1929–42
- Hadad M A, González-Reyes Á, Roig F A, Matskovsky V and Cherubini P 2021 Tree-ring-based hydroclimatic reconstruction for the northwest Argentine Patagonia since 1055 CE and its teleconnection to large-scale atmospheric circulation *Glob. Planet. Change* **202** 103496
- Henley B J, Gergis J, Karoly D J, Power S, Kennedy J and Folland C K 2015 A tripole index for the interdecadal Pacific oscillation *Clim. Dyn.* **45** 3077–90
- Hersbach H et al 2020 The ERA5 global reanalysis *Q. J. R. Meteorol. Soc.* **146** 1999–2049
- Holmes R L 1983 Computer-assisted quality control in tree-ring dating and measurement *J. Clin. Microbiol.* **18** 730–2
- Hosking J S, Orr A, Bracegirdle T J and Turner J 2016 Future circulation changes off West Antarctica: sensitivity of the Amundsen sea low to projected anthropogenic forcing *Geophys. Res. Lett.* **43** 367–76
- Kannenberg S A, Novick K A, Alexander M R, Maxwell J T, Moore D J P, Phillips R P and Anderegg W R L 2019 Linking drought legacy effects across scales: from leaves to tree rings to ecosystems *Glob. Change Biol.* **25** 2978–92
- Kendall M G 1975 *Rank Correlation Methods* 4th edn (Charles Griffin)
- Kostić S, Wagner W, Orlović S, Levanić T, Zlatanov T, Goršić E, Kesić L, Matović B, Tsvetanov N and Stojanović D B 2021 Different tree-ring width sensitivities to satellite-based soil moisture from dry, moderate and wet pedunculate oak (*Quercus robur* L.) stands across a southeastern distribution margin *Sci. Total Environ.* **800** 149536
- LeQuesne C, Acuña C, Boninsegna J A, Rivera A and Barichivich J 2009 Long-term glacier variations in the Central Andes of Argentina and Chile, inferred from historical records and tree-ring reconstructed precipitation *Palaeogeogr. Palaeoclimatol. Palaeoecol.* **281** 334–44
- LeQuesne C, Stahle D W, Cleaveland M K, Therrell M D, Aravena J C and Barichivich J 2006 Ancient austrocedrus tree-ring chronologies used to reconstruct central Chile precipitation variability from a.d. 1200 to 2000 *J. Clim.* **19** 5731–44
- Lucas C, Nguyen H and Timbal B 2012 An observational analysis of Southern Hemisphere tropical expansion *J. Geophys. Res.* **117** D17112
- Mann H B 1945 Non-parametric tests against trend *Econometrica* **13** 163–71
- Marshall G J 2003 Trends in the Southern annular mode from observations and reanalyses *J. Clim.* **16** 4134–43
- Masiokas M H, Cara L, Villalba R, Pitte P, Luckman B H, Toum E, Christie D A, Le Quesne C and Maugot S 2019 Streamflow variations across the Andes (18°–55°S) during the instrumental era *Sci. Rep.* **9** 17879
- Matskovsky V, Venegas-González A, Garreaud R, Roig F A, Gutiérrez A G, Muñoz A A, Le Quesne C, Klock K and Canales C 2021 Tree growth decline as a response to projected climate change in the 21st century in Mediterranean mountain forests of Chile *Glob. Planet. Change* **198** 103406
- McDowell N G et al 2020 Pervasive shifts in forest dynamics in a changing world *Science* **368** eaaz9463
- McNally A, Arsenault K, Kumar S, Shukla S, Peterson P, Wang S, Funk C, Peters-Lidard C D and Verdin J P 2017 A land data assimilation system for sub-Saharan Africa food and water security applications *Sci. Data* **4** 1
- Meko D 1997 Dendroclimatic reconstruction with time varying predictor subsets of tree indices *J. Clim.* **10** 687–96
- Michaelsen J 1987 Cross-validation in statistical climate forecast models *J. Appl. Meteorol. Climatol.* **26** 1589–600
- Miralles D G, Teuling A J, van Heerwaarden C C and Vilà-guerau de Arellano J 2014 Mega-heatwave temperatures due to combined soil desiccation and atmospheric heat accumulation *Nat. Geosci.* **7** 5
- Miranda A et al 2023 Widespread synchronous decline in a Mediterranean forest driven by accelerated aridity *Nat. Plants* **9** 1810–7
- Miranda A, Lara A, Altamirano A, Di Bella C, González M E and Julio Camarero J 2020 Forest browning trends in response to drought in a highly threatened mediterranean landscape of South America *Ecol. Indic.* **115** 106401
- Mishra A K and Singh V P 2010 A review of drought concepts *J. Hydrol.* **391** 202–16
- Mittermeier R A, Turner W R, Larsen F W, Brooks T M and Gascon C 2011 Global biodiversity conservation: the critical role of hotspots *Biodiversity Hotspots: Distribution and Protection of Conservation Priority Areas E F E* Zachos and J C Habel ed (Springer) pp 3–22
- Montecinos A and Aceituno P 2003 Seasonality of the ENSO-related rainfall variability in central Chile and associated circulation anomalies *J. Clim.* **16** 281–96
- Montoya-Tangarife C, Barrera F D L, Salazar A and Inostroza L 2017 Monitoring the effects of land cover change on the supply of ecosystem services in an urban region: a study of Santiago-Valparaíso, Chile *PLoS One* **12** e0188117
- Morales M S et al 2020 Six hundred years of South American tree rings reveal an increase in severe hydroclimatic events since mid-20th century *Proc. Natl Acad. Sci. USA* **117** 16816–23
- Muñoz A A et al 2020 Water crisis in Petorca Basin, Chile: the combined effects of a mega-drought and water management *Water* **12** 3
- Muñoz A A, Barichivich J, Christie D A, Dorigo W, Sauchyn D, González-Reyes Á, Villalba R, Lara A, Riquelme N and González M E 2014 Patterns and drivers of *Araucaria araucana* forest growth along a biophysical gradient in the northern Patagonian Andes: linking tree rings with satellite observations of soil moisture *Aust. Ecol.* **39** 158–69
- Myers N, Mittermeier R A, Mittermeier C G, da Fonseca G A B and Kent J 2000 Biodiversity hotspots for conservation priorities *Nature* **403** 853–8
- Nguyen H, Evans A, Lucas C, Smith I and Timbal B 2013 The Hadley circulation in reanalyses: climatology, variability and change *J. Clim.* **26** 3357–76
- Nguyen H, Lucas C, Evans A, Timbal B and Hanson L 2015 Expansion of the Southern Hemisphere Hadley cell in response to greenhouse gas forcing *J. Clim.* **28** 8067–77
- Palmer J G, Cook E R, Turney C S M, Allen K, Fenwick P, Cook B I, O'Donnell A, Lough J, Grierson P and Baker P 2015 Drought variability in the eastern Australia and New Zealand summer drought atlas (ANZDA, CE 1500–2012) modulated by the Interdecadal Pacific Oscillation *Environ. Res. Lett.* **10** 124002

- Piticar A 2018 Changes in heat waves in Chile *Glob. Planet. Change* **169** 234–46
- Quintana J M and Aceituno P 2012 Changes in the rainfall regime along the extratropical west coast of South America (Chile): 30–43° S *Atmósfera* **25** 1–22
- R Core Team 2020 *R: A language and environment for statistical computing* R Foundation for Statistical Computing, Vienna, Austria (available at: <https://www.R-project.org/>)
- Rivera J A, Penalba O C, Villalba R and Araneo D C 2017 Spatio-temporal patterns of the 2010–2015 extreme hydrological drought across the Central Andes, Argentina *Water* **9** 9
- Roco L, Engler A, Bravo-Ureta B E and Jara-Rojas R 2015 Farmers' perception of climate change in mediterranean Chile *Reg. Environ. Change* **15** 867–79
- Ropelewski C F and Jones P D 1987 An extension of the Tahiti–Darwin Southern oscillation index *Mon. Weather Rev.* **115** 2161–5
- Sarricolea P, Herrera-Ossandon M and Meseguer-Ruiz Ó 2017 Climatic regionalisation of continental Chile *J. Maps* **13** 66–73
- Schneider-Valenzuela I, Brito-Escudero C, Aguilera-Betti I, Klock-Barría K, Celis-Diez J L, Ugalde A and Muñoz A 2023 Soluciones de base Natural (SbN) para conflictos de escasez hídrica en la Ecorregión Mediterránea de Chile *Revista de Geografía Norte Grande* **85**
- Schulman E 1956 *Dendroclimatic changes in semiarid America* (University of Arizona Press)
- Schulz J J, Cayuela L, Echeverría C, Salas J and Rey Benayas J M 2010 Monitoring land cover change of the dryland forest landscape of Central Chile (1975–2008) *Appl. Geogr.* **30** 436–47
- Schwabe K, Albiac J, Connor J D, Hassan R M and Meza González L (ed) 2013 *Drought in Arid and Semi-Arid Regions: A Multi-Disciplinary and Cross-Country Perspective* (Springer) (<https://doi.org/10.1007/978-94-007-6636-5>)
- Smith-Ramírez C et al 2023 Ecosystem services of Chilean sclerophyllous forests and shrublands on the verge of collapse: a review *J. Arid Environ.* **211** 104927
- Thomte L, Bhagabati A K and Shah S K 2022 Soil moisture-based winter-spring drought variability over West Karbi Anglong region, Assam, Northeast India using tree-rings of Pinus kesiya *Environ. Chall.* **7** 100512
- Trenberth K E 1997 The definition of El Niño *Bull. Amer. Meteor. Soc.* **78** 2771–7
- Uribe S V, Estades C F and Radeloff V C 2020 Pine plantations and five decades of land use change in central Chile *PLoS One* **15** e0230193
- Urrutia-Jalabert R, González M E, González-Reyes Á, Lara A and Garreaud R 2018 Climate variability and forest fires in central and south-central Chile *Ecosphere* **9** e02171
- Venegas-González A, Juñent F R, Gutiérrez A G and Filho M T 2018 Recent radial growth decline in response to increased drought conditions in the northernmost Nothofagus populations from South America *For. Ecol. Manag.* **409** 94–104
- Venegas-González A, Muñoz A A, Carpintero-Gibson S, González-Reyes A, Schneider I, Gipolou-Zuñiga T, Aguilera-Betti I and Roig F A 2023 Sclerophyllous forest tree growth under the influence of a historic megadrought in the mediterranean ecoregion of Chile *Ecosystems* **26** 344–61
- Venegas-González A, Roig F A, Peña-Rojas K, Hadad M A, Aguilera-Betti I and Muñoz A A 2019 Recent consequences of climate change have affected tree growth in distinct *Nothofagus macrocarpa* (DC.) FM Vaz & Rodr age classes in Central Chile *Forests* **10** 653
- Villalba R, Luckman B H, Boninsegna J, D'Arrigo R D, Lara A, Villanueva-Díaz J and Pastur G M 2011 Dendroclimatology from regional to continental scales: Understanding regional processes to reconstruct large-scale climatic variations across the Western Americas *Dendroclimatology: Progress and prospects* pp 175–227
- Willamayor J, Khodri M, Villalba R and Daux V 2022 Causes of the long-term variability of southwestern South America precipitation in the IPSL-CM6A-LR model *Clim. Dyn.* **57** 2391–415
- Waugh D, Garfinkel C I and Polvani L 2015 Drivers of the recent tropical expansion in the Southern Hemisphere: changing SSTs or Ozone Depletion? *J. Clim.* **28** 6581–6
- Weisberg S 1985 *Applied Linear Regression* (Wiley)
- Wigley T M L, Briffa K R and Jones P D 1984 On the average value of correlated time series, with applications in dendroclimatology and hydrometeorology *J. Appl. Meteorol. Climatol.* **23** 201–13
- Wilks D S 2011 *Statistical Methods in the Atmospheric Sciences (International Geophysics Series)* vol 100, 3rd edn (Academic)
- Williams A P, Cook E R, Smerdon J E, Cook B I, Abatzoglou J T, Bolles K, Baek S H, Badger A M and Livneh B 2020 Large contribution from anthropogenic warming to an emerging North American megadrought *Science* **368** 314–8
- Wilson R et al 2016 Last millennium northern hemisphere summer temperatures from tree rings: part I: the long term context *Quat. Sci. Rev.* **134** 1–18
- Wilson R, Wiles G, D'Arrigo R and Zweck C 2007 Cycles and shifts: 1,300 years of multi-decadal temperature variability in the Gulf of Alaska *Clim. Dyn.* **28** 425–40